BEST AVAILABLE IMAGES

Defective images within this document are accurate representations of the original documents submitted by the applicant.

Defects in the images may include (but are not limited to):

- BLACK BORDERS
- TEXT CUT OFF AT TOP, BOTTOM OR SIDES
- FADED TEXT
- ILLEGIBLE TEXT
- SKEWED/SLANTED IMAGES
- COLORED PHOTOS
- BLACK OR VERY BLACK AND WHITE DARK PHOTOS
- GRAY SCALE DOCUMENTS

IMAGES ARE BEST AVAILABLE COPY.

As rescanning documents *will not* correct images, please do not report the images to the Image Problem Mailbox.

Improved Coagulation with Saline Solution Pretreatment during Radiofrequency Tumor Ablation in a Canine Model

Muneeb Ahmed, MD, S. Melvyn Lobo, MD, Joseph Weinstein, Jonathan B. Kruskal, MD, PhD, G. Scott Gazelle, MD, PhD, Elkan F. Halpern, PhD, S. Karim Afzal, BA, Robert E. Lenkinski, PhD, and S. Nahum Goldberg, MD

PURPOSE: To determine whether pretreatment with local NaCl injection can increase radiofrequency (RF)-induced coagulation in a large animal model.

MATERIAL AND METHODS: Multiple canine venereal sarcomas (n = 25) were implanted subcutaneously in eight mildly immunosuppressed dogs (25 mg/kg cyclosporin A twice daily). Tumors were incubated for 8–12 weeks to a diameter of 4.2–6.3 cm (5.1 cm ± 0.7). Internally cooled RF ablation (1-cm tip; 12 min; pulsed technique; 2,000-mA maximum) was performed. Tumors were pretreated with 6 mL of 18%, 24%, or 36% NaCl injected intratumorally under direct ultrasound guidance after RF electrode insertion, and this treatment was compared to RF treatment without NaCl injection and to 36% NaCl injection without RF ablation. Impedance measurements and remote thermometry were performed. These measurements and resultant coagulation were compared.

RESULTS: Significantly greater RF heating (73°C ± 11°C at 20 mm) was observed when the tumors were treated with 24% or 36% NaCl pretreatment, compared to the 47°C ± 5°C observed when 18% or no NaCl was injected ($P < .02$). In the 36% NaCl group, the entire tumor (5.2 cm ± 0.8 diameter) was completely ablated in every case, with coagulation extending several centimeters into the surrounding tissues. By comparison, control tumors (without NaCl injection) contained coagulation measuring 3.1 cm ± 0.2, surrounded by viable, well-perfused tumor ($P < .01$), and 36% NaCl alone produced 2.7 cm ± 0.6 of patchy necrosis.

CONCLUSIONS: Pretreatment with intratumoral injection of small volumes of highly concentrated NaCl markedly increases RF heating and coagulation in a large animal tumor model. The complete destruction of tumors 5 cm in diameter or larger suggests that this substantial increase may be achieved for tumor ablation in clinical practice.

Index terms: Neoplasms, therapy • Radiofrequency (RF) ablation

J Vasc Interv Radiol 2002; 13:717–724

Abbreviation: RF = radiofrequency

THERE has been marked interest in image-guided radiofrequency (RF) tumor ablation as a minimally invasive thermal therapy, particularly for focal metastatic and primary liver tumors, given the significant morbidity and mortality of standard surgical resection and the high number of patients who cannot tolerate such radical surgery (1–5). These techniques have also received increased attention for the treatment of neoplasms in other sites, including the lung (6), breast (7), brain (8), bone (9,10), kidney (11), and retroperitoneum (12). Although RF has been successful in ablating small (<3 cm) neoplasms, further optimization of ablation technique is required to induce the larger volumes of coagulation necessary to adequately treat larger tumors (13–14).

One potential strategy to increase the efficacy of RF ablation is to modulate the biologic environment of treated tissues (14). Along these lines, several investigators have demonstrated the possibility of increasing RF tissue heating and coagulation during RF ablation by altering electrical and/or thermal conduction by injecting concentrated NaCl solution into the tissues during RF application (15–17). For example, Goldberg et al (18) found that they could increase coagulation area from 3 cm to 7 cm in nor-

From the Department of Radiology (M.A., S.M.L., J.W., J.B.K., S.K.A., R.E.L., S.N.G), Beth Israel Deaconess Medical Center, Harvard Medical School, and Department of Radiology (G.S.G., E.F.H.), Massachusetts General Hospital, Boston, Massachusetts. Received February 22, 2002; revision requested March 26; revision received and accepted March 27. Address correspondence to S.N.G., Department of Radiology, Beth Israel Deaconess Medical Center, Harvard Medical School, 330 Brookline Ave., Boston, MA 02215; E-mail: sgoldber@caregroup.harvard.edu

mal in vivo porcine liver by pretreating tissues with small volumes of highly concentrated NaCl. However, nonlinear volume and concentration dependence suggested that optimum injection concentration and volume likely differ with variation in RF probe and generator design and, more importantly, with different tissues such as tumors (18).

The problem of directly translating these results to tumor ablation is further complicated by the known high interstitial pressures and heterogenicity of tumors, which limit and retard diffusion of even directly injected fluids (19). Hence, although efforts have been made to characterize the effects of NaCl pretreatment for RF ablation in normal tissues and phantom models, further work is needed to determine feasibility of this approach in tumors and optimize this phenomenon for actual tumor environments (20). We therefore conducted a series of experiments in an attempt to better characterize the direct effects of NaCl solution on local tissue electrical conductivity, RF energy deposition, and heating in a large animal model—canine venereal sarcoma. Through these experiments, we sought to optimize the effects of NaCl concentration on RF ablation (ie, tissue heating and induced coagulation) in this subcutaneous tumor model.

MATERIALS AND METHODS

Animal Studies

Approval of the institutional subcommittee on animal research care was obtained before initiation of these studies. Experiments were performed with use of a well-characterized, established canine venereal sarcoma cell line (21). Eight female Labrador dogs (retired breeders, 30–40 kg) were mildly immunosuppressed (25 mg/kg cyclosporin A twice daily; Neoral; Novartis, East Hanover, NJ) for 5 days before tumor transplantation and immunosuppression was continued until the end of the experiment. Fresh tumor (measuring approximately 2 cm in diameter) was initially harvested from a live carrier. Within 30 minutes of this tumor explantation, the tumor was homogenized with a tissue grinder with use of aseptic technique and suspended in 15 mL of Dulbecco Modified Eagle medium. Earlier control experiments have documented that this produces a concentration of approximately 1×10^7 tumor cells per 0.1 mL.

All animals were anesthetized for 30 minutes with a single dose of Telazol (12 mg/kg; Fort Dodge, Madison, NJ) before tumor transplantation. Before tumor inoculation, sites of injection were shaved, followed by disinfection with 1% povidone iodine and 70% ethanol. Under direct visualization, 1 mL of the tumor suspension was injected slowly via an 18-gauge needle into the selected tumor site. In an attempt to maximize the usable tumor yield for each animal, 12 tumors were implanted subcutaneously on the back ($n = 6$) and abdomen ($n = 6$) in each animal, for a total of 72 attempted tumor implantations.

Animals were monitored weekly to measure tumor growth. Solid, nonnecrotic tumors (as determined by ultrasound [US]) measuring 4.2–6.3 cm (5.1 cm ± 0.7) in diameter were used for ablation studies. Tumors were grown for 12–14 weeks until the desired size was achieved. Although each animal had 12 tumors implanted, variation in tumor size growth permitted that only 3–4 tumors were used from each animal (**Fig 1**). In total, 20 tumors were used in this study.

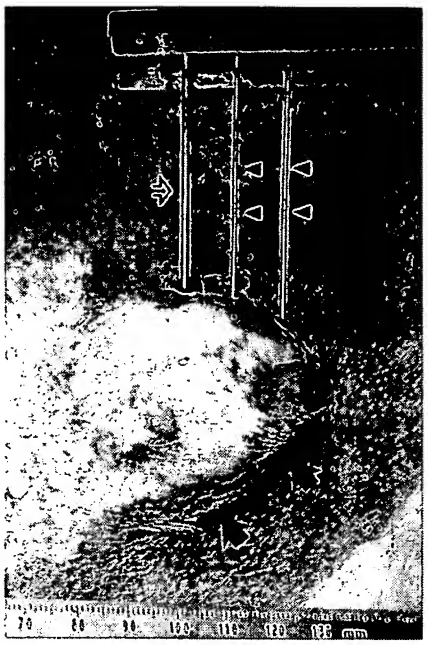

Figure 1. Subcutaneous canine venereal sarcoma tumor model. A 4.5-cm tumor is seen growing within the subcutaneous breast tissue of a female dog (large arrows). An RF electrode has been introduced into the center of the tumor (open arrow). Two thinner temperature probes have been inserted into the tumor 10 mm and 20 mm from the electrode (arrowheads). These thermocouples enable remote thermometry during RF ablation.

Experimental Design

For the ablation experiments, animals were intubated and anesthesia was maintained with isoflurane (1%–4%). Cardiac and respiratory parameters and arterial blood gases were monitored throughout the procedures. Three representative NaCl concentrations (18%, 24%, and 36%) were compared to RF ablation with no saline solution. These concentrations were selected based on earlier work with in vivo porcine liver models that demonstrated that the peak and most active range of variability occurred with a pretreatment NaCl concentration between 18% and 36% (18). As per earlier studies, the initial desired volume ranged from 0 to 25 mL. However, based on initial unpublished pilot data, only a 6-mL injection volume was used. Because of the tissue architecture and the fibrous nature of this particular tumor model, saline solution reflux from the injection site occurred when injection volumes were greater than 6 mL. As a result, we limited this study to injection of 6 mL of NaCl. Five trials each were performed for each of the four concentrations of NaCl for a total of 20 RF tumor ablations. For these experiments, tissue conductivity was first altered with NaCl, RF was applied, and temperatures and size of coagulation were measured and compared. Additionally, five tumors, serving as non-RF controls, were injected with 6 mL of 36% NaCl, for a total number of 25 treated tumors.

Alteration and Measurement of Tissue Electrical Conductivity

Tissue electrical conductivity was altered by the direct injection of NaCl solution into the tissue. Before the application of RF energy, 6 mL of NaCl (18%, 24%, or 36%) was injected into the liver tissue surrounding the elec-

Ablation Parameters for RF with Varied Concentrations of NaCl Pretreatments

% Saline	Current (A)	Power (W)	Impedance (Ω)	Temperature (°C) at 10 mm	Temperature (°C) at 20 mm	Coagulation (cm)	Total Coagulation	
							N	(%)
36 (no RF)	N/A	N/A	N/A	N/A	N/A	2.7 ± 0.6	0	0
None	0.71 ± 0.40	64 ± 25	83 ± 5	47.9 ± 13.1	47.3 ± 5.0	3.1 ± 0.2	0	0
18	1.18 ± 0.24	97 ± 27	72 ± 20	64.9 ± 10.4	50.6 ± 6.5	3.6 ± 0.7	0	0
24	1.46 ± 0.35	137 ± 9	65 ± 19	81.4 ± 18.8	64.7 ± 18.4	4.2 ± 0.9	2	40
36	1.97 ± 0.02	177 ± 62	50 ± 5	82.2 ± 13.7	73.0 ± 11.1	5.2 ± 0.8	5	100

trode with use of a 25-gauge needle under US guidance. To ensure a uniform local distribution of solution, injections were performed over the course of 30–60 seconds with the injection needle touching the previously inserted RF electrode, and with the needle slowly withdrawn along the electrode axis during injection under direct visualization with US.

Alterations in tissue electrical conductivity were measured with use of direct local impedance measurements at 500 kHz between the 1-cm-tip RF electrode and a second 2-cm-tip 21-gauge electrode placed 2 cm from the initial electrode. This standardized measurement of local impedance over this short distance with use of these well-defined parameters was performed to minimize the possible confounding effects of measuring the global system impedance that can vary as a result of extraneous variables such as grounding pad contact and nonuniform grounding-pad-to-electrode distance (22). Local tissue impedance was measured at baseline and after every NaCl injection.

Radiofrequency Application

RF was applied with use of a 500-kHz RF generator. To complete the electrical circuit, four foil grounding pads (400 cm^2 total surface area) were affixed to the lower back and thighs of the dog. With use of US guidance, a 1-cm-tip internally-cooled RF electrode was inserted into the subcutaneous tumor. Each tumor underwent a single RF ablation procedure.

RF was applied for 12 minutes at an initial generator output of 2,000 mA (200 W). If impedance increases were observed, current output was automatically reduced according to a previously designed pulsing algorithm that optimizes energy deposition and tissue coagulation (23). Parameters of the RF ablation were recorded at baseline and thereafter at 60-second intervals for the duration of RF application.

Temperature Measurements

Tissue temperatures were measured during RF application at the electrode surface and 10 and 20 mm from the electrode with use of the thermocouple probes described for use in the normal liver (18). An acrylic guide and US guidance ensured proper spacing of these temperature sensors. Additionally, the position of the temperature sensors within the tissue was adjusted along the z axis, parallel to the electrode, during the initial 3 minutes of RF application to determine and permit monitoring at the maximum temperature.

Assessment of Coagulation Necrosis (Pathologic Studies)

Animals were killed within 30 minutes after ablation treatments with pentobarbital overdose (Nembutal 0.2 mL/kg; Abbott Laboratories, North Chicago, IL). In three animals, 2 mL/kg of 2% Evans Blue were administered intravenously 15 minutes before sacrifice. The use of this agent permitted the confirmation of absent perfusion within the tumor (24). RF lesions were excised and sectioned and the extent of visible coagulation at gross pathology was measured with calipers as previously described (18,22). Specimens were sectioned along the longitudinal and transverse axes of each lesion. Measurement of the coagulation diameter perpendicular to the electrode axis was based on consensus of two observers (S.N.G. and M.A.). Histopathologic studies included cross-sectional mounting with hematoxylin and eosin staining and staining for mitochondrial enzyme activity by incubating thin representative tissue sections for 30 minutes in 2% 2,3,5-triphenyl tetrazolium chloride at 20–25°C. This latter test is capable of determining irreversible cellular injury during early stages of RF-induced necrosis (25,26).

Statistical Analysis

Tissue temperatures generated and the diameter of coagulation necrosis induced with each set of parameters were compared. Coagulation diameter was chosen as our primary measure of treatment effect because it indicates the size of tumor potentially treatable with RF. Results were subjected to statistical analysis including multiple regression analysis with interactions (including calculation of Pearson coefficient) to determine the impact of saline concentration on necrosis size and tissue temperatures. The Dunnett test was used to compare changes in impedance between the control and experimental groups.

RESULTS

A significant decrease in starting impedance was observed for trials in which 24% or 36% NaCl was injected as compared to control trials. A concurrent increase in current deposition (mA) was demonstrated with increases in NaCl concentration (Pearson coefficient = .86). Injection with 36% NaCl permitted current deposition that was significantly greater than any other NaCl concentration ($P < .01$; **Table**). Similarly, significantly more power (watts) was deposited in tu-

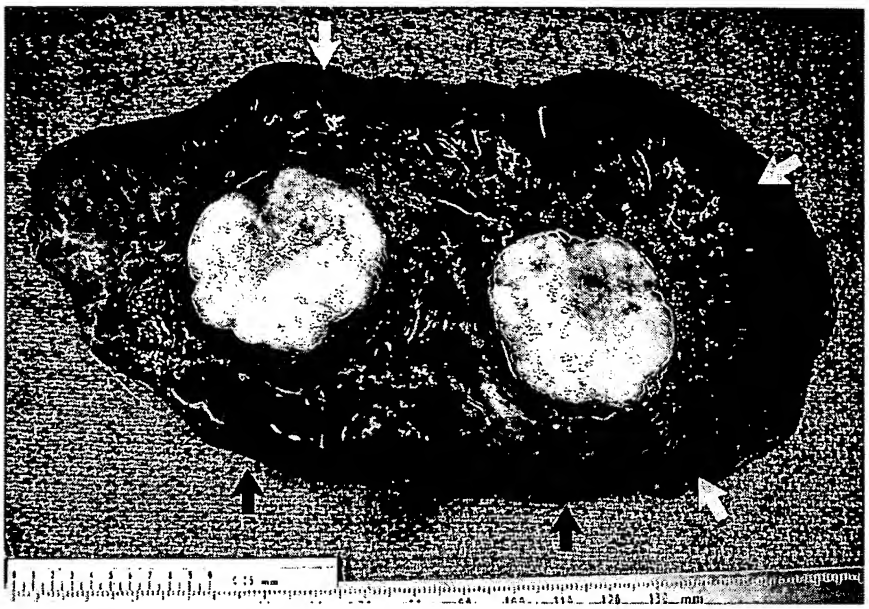

Figure 2. Completely ablated tumor after 36% NaCl pretreatment. This gross pathologic specimen is a bivalved section of a 5.5-cm dog tumor (white central regions). In addition to complete ablation of the entire tumor (as subsequently documented by staining for mitochondrial enzyme function), there is marked extension of thermal damage beyond the tumor margin. This includes liquefied fat (black arrows) as well as a wide rim of hyperemia (white arrows) at a minimum of 1 cm from the peripheral margin of the tumor.

mors injected with either 24% or 36% NaCl than in control tumors ($P < .01$).

No significant difference in temperature was observed 10 mm from the tip between any of the groups. However, significantly greater RF heating was observed 20 mm from the electrode with the introduction of increasingly greater concentrations of NaCl before RF ablation ($P = .01$; Pearson coefficient = .64). Whereas there was no difference between temperatures with no NaCl pretreatment and with injection of 18% NaCl, temperatures 20 mm from the tip of the RF probe were higher for tumors injected with 24% and 36% NaCl pretreatment (73°C ± 11) than when no NaCl was injected (47°C ± 5; $P < .02$; **Table**). Additionally, we also observed an "edge effect" of 5–15°C at the interface between tumor tissue and surrounding subcutaneous fat in four tumors in which higher NaCl injection concentrations were used (one 24% and three 36%). These temperatures were higher than measurements at 10- and 20-mm distances adjacent to the tip.

The diameter of coagulation necrosis induced by RF administration correlated with the increasing NaCl injection concentration (Pearson coefficient = .56; $P < .01$). For the group injected with 36% NaCl, the entire tumor (5.2 cm ± 0.8 diameter) was completely ablated in all five cases, with coagulation extending several centimeters into the surrounding subcutaneous and underlying muscle tissue (**Fig 2**). In the 24% NaCl group, 40% of tumors ($n = 2$) were completely ablated. By comparison, control tumors (without NaCl injection) contained coagulation measuring 3.1 cm ± 0.2 surrounded by viable, well-perfused tumor ($P < .01$). No tumors treated without pretreatment or 18% NaCl were completely ablated. By comparison, non-RF control tumors injected with 36% NaCl also exhibited irregular zones of patchy, incomplete coagulation measuring 2.7 cm ± 0.6.

In tumors that were completely treated, Evans Blue infusion for vascular staining revealed an absence of perfusion (**Fig 3**). An intense 1–2-cm zone of hyperemia surrounded this area of destruction. However, in incompletely treated tumors, residual perfusion was demonstrated. Similarly, mitochondrial enzyme function was absent throughout completely ablated tumors with normal stain uptake throughout regions of unablated tumor (**Fig 4**).

DISCUSSION

Percutaneous RF ablation is gaining increasing acceptance as a minimally invasive therapy for the treatment of primary and secondary liver cancer (27). Advantages of this thermal technique over surgical resection include reduced morbidity and the ability to induce reproducible volumes of coagulation necrosis for tumors smaller than 3 cm in diameter (13–14). However, several clinical studies have pointed to inadequate and variable treatment of focal liver lesions greater than 3.5 cm in diameter (5,28). Even optimistic reports of percutaneous RF ablation of colorectal liver metastases note local tumor recurrence in 35% of cases (3), and a recent study reports that a majority of hepatocellular carcinomas measuring greater than 5 cm are incompletely treated with current thermal ablation strategies (5,28,29). Clearly, there remains a need to further develop means to improve the reliability of RF ablation in larger liver tumors.

The "Bio-heat" equation describing RF induced heat transfer through tissue, previously expressed by Pennes et al (30), has been further simplified by Goldberg et al (14) to:

coagulation necrosis = energy deposited × local tissue interactions − heat loss

Based on this, much attention has centered on increasing RF-induced coagulation volume by altering these factors. Initial efforts focused on increasing the RF coagulation zone with use of multiple probes simultaneously, cooled-tip probes, and pulsed RF energy in an attempt to increase overall energy deposition (24,31,32), but this approach by itself has not produced the desired outcome of increased tumor destruction, given biologic limitations to high current deposition and tissue physiology (such as blood flow and poor thermal conductivity) that limit the effectiveness of increased energy deposition for in vivo coagulation. However, recent work has centered on altering ei-

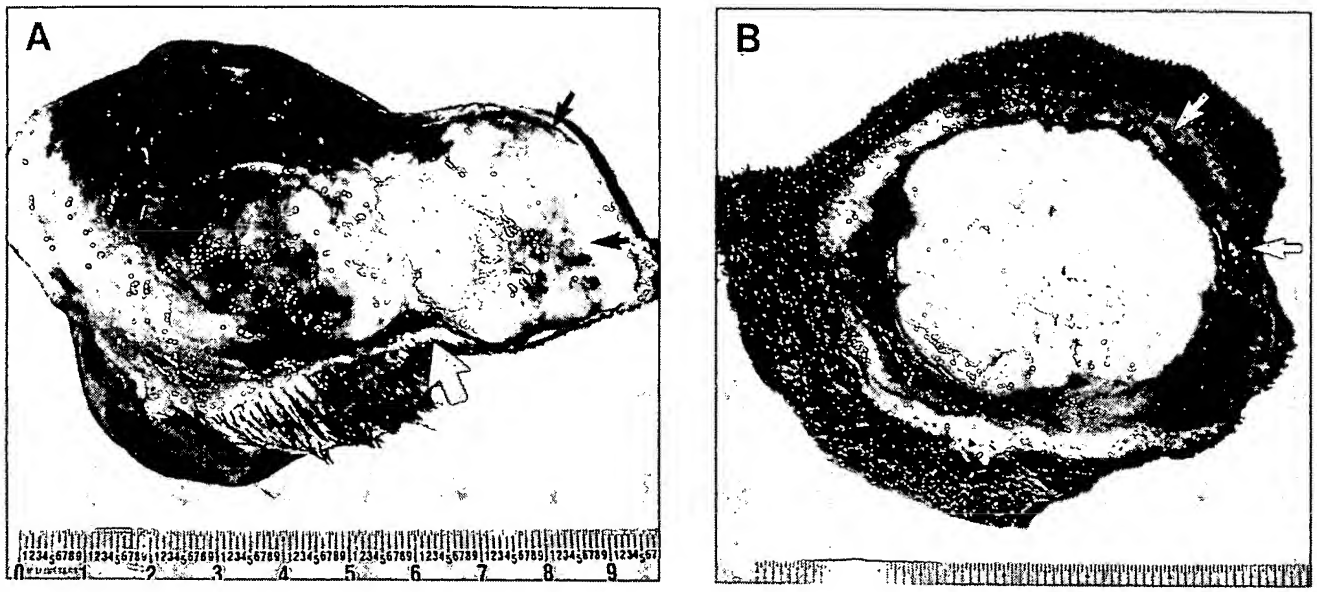

Figure 3. Effect of NaCl pretreatment on vascular perfusion after RF ablation. **(A)** Tumor was treated with RF ablation alone and demonstrates a 3.2-cm central focus of coagulation (large white arrow) with marked hyperemia surrounding this zone. Additionally, Evans Blue, a marker for vascular perfusion, intensely stains the peripheral subcutaneous tissues and residual unablated tumor (black arrows). **(B)** This 5.5-cm tumor treated with RF ablation and 36% NaCl solution pretreatment shows no evidence of residual vascular perfusion. Intense hyperemia/perfusion is seen in the cutaneous and peripheral tissues (white arrows). However, no evidence of mitochondrial enzyme activity or perfusion was seen in this completely ablated tumor.

ther local tissue characteristics such as electrical conductivity or altering blood flow with use of adjuvants as a means for improving RF ablation results for equivalent RF energy output (33,34).

Two mechanisms have been proposed to account for the improved tissue heating and increased RF-induced coagulation with simultaneous NaCl infusion: (i) that NaCl alters tissue properties such as electrical conductivity to permit greater RF energy deposition, or (ii) that the injection of fluid during RF application improves the thermal conduction within the tissues by more rapidly and effectively spreading heat by convection over a larger tissue volume. The injection of adjuvant NaCl solution with RF ablation has been shown to increase RF energy deposition by flattening the heat distribution curve, permitting greater energy delivery with less tissue boiling. With this technique, Curley and Hamilton (15) infused as much as 10 mL/min of normal 0.9% saline solution in ex vivo liver for 4 minutes during RF application to increase the coagulation diameter from 1.4 cm to 2.6 cm. Livraghi et al (16) also reported increasing coagulation diameter to 4.1 cm with use of continuous infusion of normal saline solution at 1 mL/min in experimental animal models and human liver tumors (16). With use of a "cooled-wet" electrode, Miao et al (35,36) infused 1 mL/min of 5% hypertonic saline solution in ex vivo liver for 12 minutes during RF application and achieved coagulation measuring 6.0 cm in diameter.

Goldberg et al (18) explored the relationship between NaCl injection and RF energy deposition in both phantom agar models and in vivo porcine liver, establishing that much of the increase in coagulation necrosis reported by investigators can be attributed to altered tissue conductivity. With use of a simplex optimization strategy, their study demonstrated the need for high NaCl concentration if maximal coagulation is to be achieved. Further study in ex vivo agar phantoms and in vivo normal porcine liver has enabled mathematic modeling and determination of the equations governing heat distribution within varying tissue types, permitting greater predictability for heterogeneous models (20). The current study brings this strategy closer to clinical implementation by corroborating these observations in a more clinically relevant animal tumor model.

Our study demonstrates correlation between increasing NaCl concentration and an increase in electrical conductivity, current deposition, temperature (at 10 mm and 20 mm from the electrode), and coagulation diameter. This relates well with data in normal porcine liver showing that maximum effect was seen with the injection of 6 mL of 36% NaCl, as compared to lower concentrations at the same volume (18). At those doses, we were also able to successfully destroy 5-cm tumors in a consistent and repeatable manner. This clearly demonstrates the potential for adjuvant NaCl injection as a method to increase RF-induced coagulation volumes in a reliable manner.

Ideal NaCl injection concentration for RF ablation was directly determined within the parameters of this large animal tumor model. However, we were unable to systematically study a wide range of NaCl volumes because we were able to inject only 6 mL of NaCl solution within preliminary trials in this study. Clearly, the

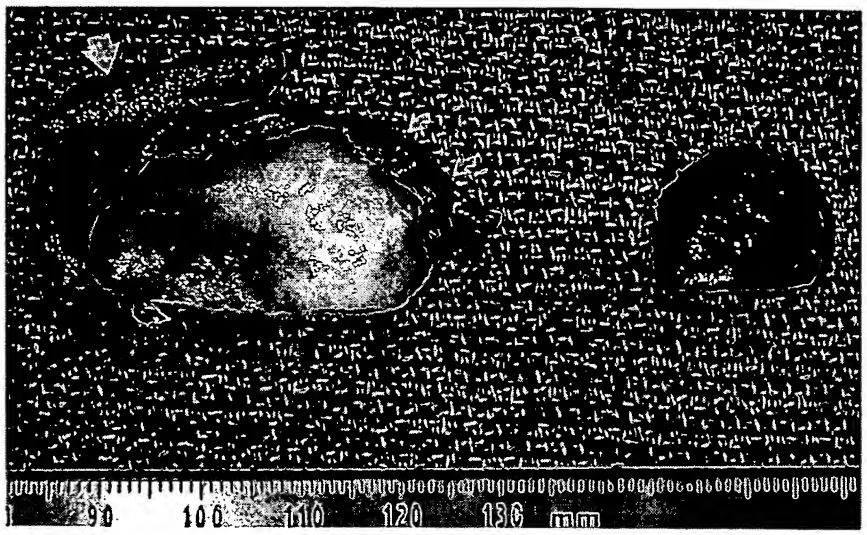

Figure 4. Effect of NaCl pretreatment on RF ablation efficacy with use of tetrazolium chloride staining. Two representative specimens are presented. On the right is a small piece of unablated control tumor that has stained intensely red, denoting normal mitochondrial activity. The specimen on the left has been sectioned from a tumor treated with RF ablation and 24% NaCl pretreatment. The white, unstained appearance denotes the absence of mitochondrial function. Additionally, ablated nonviable subcutaneous tissue is identified (large white arrow). This can be readily be distinguished from the red staining and viable subcutaneous tissue denoted by the curved arrows. This tumor was completely ablated.

results of this particular study demonstrate the sufficiency of a 6-mL volume of pretreatment NaCl solution injection for treating 5-cm tumors. Optimal necrosis occurred with this volume in the in vivo porcine liver (18). Additionally, reported results of previous studies in normal porcine liver have shown that smaller volumes (1–4 mL) produced variable alterations in tissue conductivity, even at the highest concentrations of NaCl (18). In addition, irregular distribution of larger volumes (>10 mL) results in irregular RF zones and increases the potential risk of seeding as tumor cells are carried distally by fluid (18). Interestingly, injections of 36% NaCl solution alone also induced small zones of coagulation necrosis, albeit irregular and incomplete. Indeed, high-concentration NaCl solution has been previously reported as a sclerosing agent for vascular malformations in several clinical situations (37–39). Therefore, although earlier phantom studies involving pretreatment NaCl in combination with RF ablation have demonstrated a predominant effect from altered conductivity and increased energy deposition (20), coagulation by pretreatment NaCl may also have additional benefit by eliminating blood flow immediately surrounding the RF probe, reducing perfusion-mediated vascular cooling and enabling greater necrosis (20,40).

In larger tumors, the usefulness of RF ablation has been limited by continued growth of tumors resulting from a failure to ablate an adequate surgical margin, generally accepted as 5–10 mm of seemingly normal surrounding tissue (41). Our study has clearly shown that pretreatment injection of smaller volumes of concentrated NaCl in an in vivo tumor model can not only reliably kill larger tumors, but can also treat an appropriate "surgical" margin of normal tissue. This reduces the likelihood of growth recurrence and has significant clinical implications regarding the potential of RF ablation within the scope of liver cancer treatments (41).

An "edge effect" phenomenon was observed in which the highest temperatures were observed at tumor margins in some tumors with high-concentration NaCl injection. Two reasons, an insulation effect and/or an electrical effect, are likely to account for this observation. In treating patients with cirrhosis and hepatocellular carcinoma lesions, Livraghi et al (42) described an "oven effect" in which RF-induced necrosis conformed to the size and shape of the treated tumor. They postulated that cirrhotic liver surrounding a tumor acted as a thermal insulator, facilitating thermally mediated necrosis (42). This particular animal model possesses a thick layer of subcutaneous fat that may have caused greater heat retention within the tumor. Such a mechanism was invoked by Bohm et al (43) to help account for increased RF coagulation in normal human breast and cow udder specimens. However, the fact that this "edge effect" is seen only at higher currents or with marked increases in impedance suggests that this phenomenon is based more on electrical parameters rather than an alteration in thermal conduction. NaCl pretreatment reduced the local impedance, permitting very high RF currents to reach the tumor edge and an even larger impedance differential between the tumor and the poorly conductive fatty tissue surrounding it. As such, amplification in impedance across this tissue boundary can potentially inhibit RF current transmission and increase resistive heating at the tumor margin (44). Regardless of mechanism, this effect merits further exploration, characterization, and optimization based on tumor and local tissue types.

Several limitations of this study must be addressed. First, the extremely large volumes of coagulation created may not always be beneficial or desired. Overtreatment in some cases could be detrimental if surrounding structures were damaged or if too little normal tissue is preserved to permit normal organ function. Given that we were unable to measure coagulation in all three dimensions, it is difficult to assess the true volume and ultimate shape of lesions that will be created in thicker tissues. Therefore, although we were able to completely treat tumors as large as 5 cm, it is likely that we have underestimated the tumor volume and size that could be potentially treated. Additionally, it is conceivable that the zone of necrosis will approximate an ellipsoid rather than a spherical lesion. Results may further vary in other, more clinically relevant neoplastic tissues as a result

of differences in tissue composition and blood flow. Hence, extrapolation to other types of tumors should be done with caution.

Although much work has been done to characterize and improve on RF and other methods of tumor ablation, to our knowledge, this is the first report of RF ablation in an animal tumor model of clinically relevant size. This particular model is straightforward and may be used for further large-volume tumor ablation studies with relative ease. Additional studies involving similar large animal tumor models are a welcome and necessary next step in optimizing RF ablation use by providing models that more closely represent clinical scenarios.

In conclusion, pretreatment with intratumoral injection of small volumes of highly concentrated NaCl markedly increases RF heating and coagulation in a large animal tumor model. The complete destruction of tumors measuring as large as 5 cm in diameter or larger, suggests that this substantial increase may be achieved for tumor ablation in clinical practice.

Acknowledgment: Supported by a grant from the National Cancer Institute, National Institutes of Health, Bethesda, MD (RO1-CA87992-01a1).

References

1. Gazelle GS, Goldberg SN, Solbiati L, Livraghi T. Tumor ablation with radiofrequency energy. Radiology 2000; 217:633–646.
2. Rossi S, Buscarini E, Garbagnati F, et al. Percutaneous treatment of small hepatic tumors by an expandable RF needle electrode. AJR Am J Roentgenol 1998; 170:1015–1022.
3. Solbiati L, Livraghi T, Goldberg SN, et al. Percutaneous radiofrequency ablation of hepatic metastases from colorectal cancer: long-term results in 117 patients. Radiology 2001; 221:159–166.
4. Livraghi T, Goldberg SN, Meloni F, Solbiati L, Gazelle GS. Hepatocellular carcinoma: comparison of efficacy between percutaneous ethanol instillation and radiofrequency. Radiology 1999; 210:655–661.
5. Livraghi T, Goldberg SN, Lazzaroni S, Meloni F, Ierace T, Gazelle GS. Hepatocellular carcinoma: radiofrequency ablation of medium and large lesions. Radiology 2000; 214:761–768.
6. Dupuy DE, Zagoria RJ, Akerley W, Mayo-Smith WW, Kavanaugh PV, Safran H. Percutaneous RF ablation of malignancies in the lung. AJR Am J Roentgenol 2000; 174:57–60.
7. Jefferey SS, Birdwell RL, Ikeda DM, et al. Radiofrequency ablation of breast cancer: first report of emerging technology. Arch Surg 1999; 134:1064–1068.
8. Anzai Y, Lufkin R, DeSalles A, Hamilton DR, Farahani K, Black KL. Preliminary experience with MR-guided thermal ablation of brain tumors. Am J Neuroradiol 1995; 16:39–48.
9. Rosenthal DI, Hornicek FJ, Wolfe MW, Jennings LC, Gephart MC, Mankin HJ. Changes in the management of osteoid osteoma. J Bone Joint Surg Am 1998; 80:815–821.
10. Dupuy DE, Safran H, Mayo-Smith WW, Goldberg SN. Radiofrequency ablation of painful osseous metastases [abstract]. Radiology 1998; 209(suppl): 389.
11. Gervais D, Wood B, McGovern FJ, Goldberg SN, Mueller PR. Radiofrequency ablation of renal cell carcinoma: early clinical experience. Radiology 2000; 217:665–672.
12. Lewin JS, Connell CF, Duerk JL, et al. Interactive MRI-guided radiofrequency interstitial thermal ablation of abdominal tumors: clinical trial for evaluation of safety and feasibility. J Magn Reson Imaging 1998; 8:40–47.
13. McGahan JP, Dodd GD III. Radiofrequency ablation of liver tumors: current status. AJR Am J Roentgenol 2001; 176:3–16.
14. Goldberg SN, Gazelle GS, Mueller PR. Thermal ablation therapy for focal malignancy: a unified approach to underlying principles, techniques, and diagnostic imaging guidance. AJR Am J Roentgenol 2000; 174:323–331.
15. Curley MG, Hamilton PS. Creation of large thermal lesions in liver using saline-enhanced RF ablation. In: Proceedings of the 19th International Conference of IEEE/EMBS, 1997: 2516–2519.
16. Livraghi T, Goldberg SN, Lazzaroni S, et al. Saline-enhanced radiofrequency tissue ablation in the treatment of liver metastases. Radiology 1997; 202:205–210.
17. Miao Y, Yicheng N, Stefaan M, et al. Ex vivo experiment on radiofrequency liver ablation with saline infusion through a screw-tip cannulated electrode. J Surg Res 1997; 71:19–24.
18. Goldberg SN, Ahmed M, Gazelle GS, et al. Radio-frequency thermal ablation with NaCl solution injection: effect of electrical conductivity on tissue heating and coagulation—phantom and porcine liver study. Radiology 2001; 219:157–165.
19. Jain RK. Barriers to drug delivery in solid tumors. Sci Am 1994; 271:58–65.
20. Lobo SM, Afzal K, Kruskal JB, Lenkinski RE, Gazelle GS, Goldberg SN. Radiofrequency thermal ablation using an adjuvant NaCl gel: effect of electrical conductivity on tissue coagulation [abstract]. Radiology 2001; 201(suppl): 398.
21. Koike T, Kudo T, Otomo K, Sakai T. Successively transplanted canine transmissible sarcoma. Gann 1979; 70:115–118.
22. Goldberg SN, Solbiati L, Halpern EF, Gazelle GS. Variables effecting proper system grounding for RF ablation in an animal model. J Vasc Interv Radiol 2000; 11:1069–1075.
23. Goldberg SN, Stein M, Gazelle GS, Sheiman RG, Kruskal JB, Clouse ME. Percutaneous radiofrequency tissue ablation: optimization of pulsed-RF technique to increase coagulation necrosis. J Vasc Interv Radiol 1999; 10:907–916.
24. Goldberg SN, Gazelle GS, Solbiati L, Rittman WJ, Mueller PR. Radiofrequency tissue ablation: increased lesion diameter with a perfusion electrode. Acad Radiol 1996; 3:636–644.
25. Goldberg SN, Walovitch R, Halpern EF, Gazelle GS. Immediate detection of RF induced coagulation necrosis using a novel ultrasound contrast agent. Radiology 1999; 213:438–444.
26. Goldlust EJ, Paczynski RP, He YY, Hsu CY, Goldberg MP. Automated measurement of infarct size with scanned images of triphenyltetrazolium chloride-stained rat brains. Stroke 1996; 27: 1657–1662.
27. Livraghi T. Guidelines for the treatment of liver cancer. Eur J Ultrasound 2001; 13:167–176.
28. de Baere T, Elias D, Dromain C, et al. Radiofrequency ablation of 100 hepatic metastases with a mean follow-up of more than 1 year. AJR Am J Roentgenol 2000; 175:1619–1625.
29. Livraghi T, Lazzaroni S, Meloni F. Radiofrequency thermal ablation of hepatocellular carcinoma. Eur J Ultrasound 2001; 13:159–166.
30. Pennes HH. Analysis of tissue and arterial blood temperatures in the resting human forearm. J Appl Physiol 1948; 1:93–122.
31. Goldberg SN, Gazelle GS, Dawson SL, Rittman WJ, Mueller PR, Rosenthal DI. Tissue ablation with radiofrequency: effect of probe size, gauge, duration, and temperature on lesion volume. Acad Radiol 1996; 3:212–218.
32. Lorentzen T, Christensen NE, Nolsoe CP, Torp-Pedersen ST. Radiofrequency tissue ablation with a cooled needle in vitro: ultrasonography, dose response, and lesion temperature. Acad Radiol 1997; 4:292–297.
33. Goldberg SN, Hahn PF, Halpern E, Fogle R, Gazelle GS. Radiofrequency tissue ablation: effect of pharmacologic modulation of blood flow on coagula-

tion diameter. Radiology 1998; 209:761–769.
34. Patterson EJ, Scudamore CH, Owen DA, Nagy AG, Buczkowski AK. Radiofrequency ablation of porcine liver in vivo: effects of blood flow and treatment time on lesion size. Ann Surg 1998; 227:559–565.
35. Miao Y, Ni Y, Yu J, Zhang H, Baert A, Marchal G. An ex-vivo study on radiofrequency tissue ablation: increased lesion size by using an "expandable-wet" electrode. Eur Radiol 2001; 11:1841–1187.
36. Miao Y, Ni Y, Yu J, Marchal G. A comparative study on validation of a novel cooled-wet electrode for radiofrequency liver ablation. Invest Radiol 2000; 35:138–141.
37. McCoy S, Evans A, Spurrier N. Sclerotherapy for leg telangiectasia: a blind comparative trial of polidocanol and hypertonic saline. Dermatol Surg 1999; 25:381–385.
38. Ponsky JL, Mellinger JD, Simon IB. Endoscopic retrograde hemorrhoidal sclerotherapy using 23.4% saline: a preliminary report. Gastrointest Endosc 1991; 37:155–158.
39. Puissegur Lupo ML. Sclerotherapy: review of results and complications in 200 patients. J Dermatol Surg Oncol 1989; 15:214–219.
40. Goldberg SN, Kruskal JB, Oliver BS, Clouse ME, Gazelle GS. Percutaneous tumor ablation: increased coagulation by combining radiofrequency ablation and ethanol instillation in a rat breast tumor model. Radiology 2000; 217:827–831.
41. Dodd GD, Frank MS, Aribandi M, Chopra S, Chintapalli KN. Radiofrequency thermal ablation: computer analysis of the size of the thermal injury created by overlapping ablations. AJR Am J Roentgenol 2001; 177:777–782.
42. Livraghi T, Goldberg SN, Lazzaroni S, Meloni F, Solbiati L, Gazelle GS. Small hepatocellular carcinoma: treatment with radio-frequency ablation versus ethanol injection. Radiology 1998; 210:655–661.
43. Bohm T, Hilger I, Muller W, Reichenbach JR, Fleck M, Kaiser WA. Saline-enhanced radiofrequency ablation of breast tissue: an in vitro feasibility study. Invest Radiol 2000; 35:149–157.
44. Pearce JA. Review of electrical field relation. In: Pearce JA. Electrosurgery. New York: Wiley Medical Publications, 1986;224–234.